J. Fluid Mech. (1998), *vol.* 362, *pp.* 157–176. Printed in the United Kingdom

Propagation of solitary waves through significantly curved shallow water channels

By AIMIN SHI[1], MICHELLE H. TENG[2] AND THEODORE Y. WU[3]

[1] Environmental Fluid Dynamics Research, Jamesburg, NJ 08831, USA

[2] Department of Civil Engineering, University of Hawaii at Manoa, Honolulu, HI 96822, USA

[3] Engineering Science, California Institute of Technology, Pasadena, CA 91125, USA

(Received 20 September 1996 and in revised form 18 November 1997)

Propagation of solitary waves in curved shallow water channels of constant depth and width is investigated by carrying out numerical simulations based on the generalized weakly nonlinear and weakly dispersive Boussinesq model. The objective is to investigate the effects of channel width and bending sharpness on the transmission and reflection of long waves propagating through significantly curved channels. Our numerical results show that, when travelling through narrow channel bends including both smooth and sharp-cornered 90°-bends, a solitary wave is transmitted almost completely with little reflection and scattering. For wide channel bends, we find that, if the bend is rounded and smooth, a solitary wave is still fully transmitted with little backward reflection, but the transmitted wave will no longer preserve the shape of the original solitary wave but will disintegrate into several smaller waves. For solitary waves travelling through wide sharp-cornered 90°-bends, wave reflection is seen to be very significant, and the wider the channel bend, the stronger the reflected wave amplitude. Our numerical results for waves in sharp-cornered 90°-bends revealed a similarity relationship which indicates that the ratios of the transmitted and reflected wave amplitude, excess mass and energy to the original wave amplitude, mass and energy all depend on one single dimensionless parameter, namely the ratio of the channel width b to the effective wavelength λ_e. Quantitative results for predicting wave transmission and reflection based on b/λ_e are presented.

1. Introduction

Since Scott Russell first discovered in 1834 that a solitary wave propagates without changing its shape and speed in a straight channel of uniform depth and width, the property of solitary waves in straight channels has been extensively studied by many authors. These studies include the discovery by Zabusky & Kruskal (1965) that two colliding solitary waves pass through each other without losing their identity (for which feature the term 'soliton' was coined), the analytical proof by Benjamin (1972) on the robust stability of solitary waves, and the theoretical, numerical, and experimental investigations of transmission and reflection of solitary wave propagating in straight channels of variable depth and width by Peregrine (1967), Madsen & Mei (1969), Johnson (1973), Shuto (1974), Goring (1978), Miles (1979), Chang, Melville & Miles (1979), Wu (1981), Schember (1982), Kirby & Vengayil (1988), Teng & Wu (1992, 1994), among others.

In nature and in engineering applications, rivers, harbours, and canals often have winding turns in direction, therefore it is important to understand how water waves propagate through curved channels. Thus far, only a few studies have been focused particularly on investigating the evolution of solitary waves propagating in curved channels, yet there have been useful results obtained from several related studies.

Rostafinski (1972) obtained analytical solutions based on the linear wave equations to describe the propagation of extremely long acoustic waves in smoothly curved rectangular ducts whose width was at least two orders of magnitude smaller than the wavelength. His theoretical results showed that long waves in a narrow curved line (in the limit that the duct width approaches zero) propagate as if the line was straight, while in relatively wider channels, the propagation of long waves was found to be profoundly influenced by the sharpness of the channel bend. He discovered that the distribution of the tangential fluid velocity in the transverse direction inside a narrow circular-arc bend is the same as that of a potential vortex. He also found that the phase velocity would increase proportionally to the sharpness of the bend. To study short periodic surface waves propagating in wide (with channel width about five times the wavelength) smoothly curved water channels, Kirby, Dalrymple & Kaku (1994) applied the parabolic approximation based on the linear wave equations, and their results revealed that through wide channel bends, both wave reflection and diffraction are important. In fact, the reflection of short waves was so strong that growth of a Mach stem at the outer wall of the channel bend was observed. Another interesting study was carried out by Webb & Pond (1986) who investigated theoretically (by solving the linear wave equations through separation of variables and expressing the solution with harmonic basis functions) the propagation of linear periodic long waves under the influence of the Coriolis force through smoothly curved channel bends. Several parameters, including the ratio of channel width to wavelength (which ranged from 0.03 to 0.5 in Webb & Pond's study), bending angle, bending sharpness, and Coriolis force, were found to affect the transmission and reflection of long waves through smoothly curved channel bends. Their analytical solution indicated that increasing the bend sharpness would give rise to a higher reflection coefficient. However, as the authors noted, the analytical method failed in very sharp bends such as sharp-cornered right-angled bends.

To model nonlinear waves, Katopodes & Wu (1987) developed a finite element scheme to solve the weakly nonlinear and weakly dispersive Boussinesq equations for simulation of undular bores and solitary waves propagating through channel contractions and expansions. Their study was focused on examining the accuracy and efficiency of the finite element scheme and the proper boundary conditions without discussing in detail the transmission and reflection of solitary waves through channel bends. Recently, Shi & Teng (1996) carried out numerical simulations based on Wu's (1981) generalized Boussinesq (gB) equations to study the evolution of nonlinear solitary wave through narrow curved water channels. They found that a solitary wave is almost completely transmitted with little reflection or scattering even when propagating through significantly curved narrow channels including those with 180°-bends. This result was seen to be consistent with the result found by Rostafinski (1972) for long acoustic waves in smoothly curved narrow ducts. In Shi & Teng's (1996) study, all the channels investigated had the ratio of channel width over water depth equal to one.

The present study is an extension of previous ones to investigate the propagation of solitary waves, which are shallow water long waves with well-balanced nonlinear and dispersive effects, through significantly curved rectangular channels of uniform

depth and width, with particular emphasis on examining wave propagation through sharp-cornered right-angled bends. Both wide and narrow right-angled bends are investigated by varying the channel width systematically. In addition, the propagation of solitary waves through wide smoothly curved channel bends is simulated, and the results are compared with those in sharp-cornered right-angled bends. The objective is to examine the effects of channel width, bending sharpness and wavelength on transmission and reflection of solitary waves through significantly curved channels. The present results are compared with the results obtained from the previous studies on long acoustic waves and periodic water waves in smoothly curved ducts or channels based on linear theory.

The numerical simulation in the present study is based on Wu's (1981) generalized weakly nonlinear and weakly dispersive Boussinesq equations by using the same finite difference scheme developed by Wang, Wu & Yates (1988, 1992). In our numerical simulation, the flow is assumed inviscid and incompressible, and the effects of surface tension and Coriolis force are excluded.

2. Governing equations

The generalized Boussinesq (gB) equations derived by Wu (1981, (41)–(42)) are a set of weakly nonlinear and weakly dispersive wave equations that can be used to describe the generation and propagation of shallow water long waves over variable topographies. This set of equations is generalized in the sense that it can model general wave problems where water depth may vary both in space and in time, and waves may travel in different directions simultaneously. In addition, compared with the traditional Boussinesq equations involving surface elevation and two horizontal velocity components (Katopodes & Wu 1987), Wu's gB equations are written in terms of surface elevation and velocity potential to reduce the number of unknowns and have been shown to be more efficient numerically. For the particular problem considered in the present study, namely the evolution of solitary wave propagating in curved channels of constant depth and width, the gB equations can be written for a curvilinear coordinate system as

$$\zeta_t + \frac{1}{L^2}[(1+\zeta)\phi_x]_x + [(1+\zeta)\phi_y]_y + \frac{k}{L}(1+\zeta)\phi_y = 0, \tag{1}$$

$$\phi_t + \frac{1}{2L^2}\phi_x^2 + \frac{1}{2}\phi_y^2 + \zeta - \frac{1}{3L^2}\phi_{xxt} - \frac{1}{3}\phi_{yyt} - \frac{1}{3}\frac{k}{L}\phi_{yt} = 0, \tag{2}$$

where ζ is the free-surface elevation, ϕ the depth-averaged velocity potential, and x is the boundary-fitted coordinate tangent to the inner channel wall and y is normal to x as shown in figure 1. All the variables are in non-dimensional form, with length scaled by water depth h, time by $(h/g)^{1/2}$ and velocity by $(gh)^{1/2}$, where g is the acceleration due to gravity. The typical channel bend curvature is $k = 1/R$, where R is the local radius of the inner channel wall, and the scale factor L is given by $L = 1 + ky$. The subscripts in the equations indicate the specific differentiations. In the gB model, equation (1) is the continuity equation, and equation (2) is derived from the integral of the Euler equation by using perturbation expansion to the second order.

The proper boundary conditions applied in the present study are the unperturbed condition at the far upstream and far downstream boundaries, and no-penetration condition at the channel walls, namely

$$\zeta = 0,\ \phi_x = 0,\ \text{and}\ \phi_y = 0\ \text{at}\ x = \pm\infty; \quad \phi_y = 0\ \text{at}\ y = 0,\ b, \tag{3}$$

where b is the channel width.

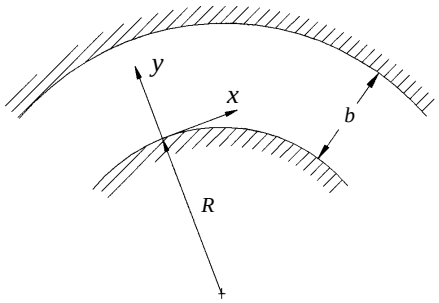

FIGURE 1. Coordinate system.

It is known that a solitary wave travels in a straight channel of uniform depth and width without changing its shape and speed. This stationary solitary wave solution to the Boussinesq equations is given by (Teng 1997)

$$\zeta(x,t) = \frac{\alpha \operatorname{sech}^2\beta(x - x_0 - ct)}{1 + \alpha \tanh^2\beta(x - x_0 - ct)}, \tag{4}$$

$$c = \left\{ \frac{6(1+\alpha)^2}{\alpha^2(3+2\alpha)}[(1+\alpha)\ln(1+\alpha) - \alpha] \right\}^{1/2} \tag{5}$$

where $\beta = [3\alpha/4(1+0.68\alpha)]^{1/2}$ and x_0 is the initial solitary wave position. The expression (5) for wave speed c is directly adopted from the original exact solution in closed form of the gB equations first solved in Teng & Wu (1992, pp. 227–229) (see also Yates 1995), while the wave profile (4) is an empirical formula (Yates 1995; Teng 1997) that gives one of the best approximations to the exact solitary wave profile based on the Boussinesq equations (Teng & Wu 1992) whose closed form is not known. This stationary solitary wave solution will be used to test the accuracy of our numerical scheme, and it will also be used as the initial condition in all our numerical simulations presented in this paper.

To examine the mass and energy conservation laws, we define the excess mass M_e of the wave system as

$$M_e = \int_{-\infty}^{+\infty} \int_0^b \zeta L \, \mathrm{d}y \, \mathrm{d}x, \tag{6}$$

and the total mechanical energy as

$$E = \int_{-\infty}^{+\infty} \int_0^b \frac{1}{2}\left[\frac{1}{L^2}\phi_x^2 + \phi_y^2 + \zeta^2\right] L \, \mathrm{d}y \, \mathrm{d}x. \tag{7}$$

Multiplying (1) with L and integrating the resulting equation over x and y, we have

$$\frac{\mathrm{d}M_e}{\mathrm{d}t} + \int_0^b \int_{-\infty}^{+\infty} \frac{1}{L}[(1+\zeta)\phi_x]_x \, \mathrm{d}x\mathrm{d}y + \int_{-\infty}^{+\infty} \int_0^b [L(1+\zeta)\phi_y]_y \mathrm{d}y\mathrm{d}x = 0$$

which gives

$$\frac{\mathrm{d}M_e}{\mathrm{d}t} = -\int_0^b \frac{1}{L}(1+\zeta)\phi_x \Big|_{-\infty}^{+\infty} \mathrm{d}y - \int_{-\infty}^{+\infty} L(1+\zeta)\phi_y \Big|_0^b \mathrm{d}x.$$

By applying the boundary conditions (3), we readily show that $\mathrm{d}M_e/\mathrm{d}t = 0$, which indicates that excess mass is conserved exactly based on the gB model. For an inviscid

wave system without external forcing, the total mechanical energy must also be conserved. Combining the results from (1) and (2), we can show that conservation of mechanical energy is also satisfied by the gB model accurately to the higher order consistent with the order of accuracy of the initial perturbation expansion in deriving the gB model from the Euler equations. This proof involves straightforward but lengthy algebraic manipulations which are omitted from our present paper for brevity. (Related derivations and discussions on energy conservation based on a section-mean Boussinesq long-wave model of the same class as the gB model can be found in Teng 1990.) Conservation of mass and mechanical energy is used as one of the criteria in our computation to monitor the accuracy and correctness of our numerical simulation.

For nonlinear long waves propagating through curved channels, there are several parameters that may affect wave transmission and reflection. These parameters include wave amplitude α, wavelength λ, channel width b, and bending sharpness a which was defined by Rostafinski (1972, 1976) as $a = 1 + kb$. For solitary waves, we define the effective wavelength λ_e as the wavelength within which the wave elevation everywhere is larger than 1% of its amplitude α. From (4), this λ_e is given by

$$\lambda_e = \frac{2}{\beta}\ln\frac{(1+0.01\alpha)^{1/2}+0.99^{1/2}}{(0.01+0.01\alpha)^{1/2}}, \tag{8}$$

which predicts that λ_e=22.2, 13.2, and 10.6 for solitary waves of amplitude $\alpha = 0.1$, 0.3, and 0.5, respectively. In our numerical simulation, the effects of the aforementioned parameters are investigated.

3. Numerical scheme

To solve the gB equations (1)–(2) numerically, we adopt a predictor–corrector finite difference scheme developed by Wang *et al.* (1988, 1992). Specifically, Euler forward is used for time derivatives and central difference is applied for spatial differentiations. We notice that since the gB equations have mixed spatial and temporal derivative terms in both horizontal directions, it can be quite complicated to solve this set of equations by using direct matrix inversion. In the present study, we adopt an iterative scheme which is relatively simple and numerically efficient as demonstrated in Wang *et al.* (1988, 1992). The detailed numerical scheme is given as follows:

$$\left.\begin{aligned} \text{predictor:}\quad & \zeta^*_{i,j} = \zeta^n_{i,j} + \Delta t E^n_{i,j}, \\ & \phi^*_{i,j} = F^*_{i,j} + \Delta t\left(1 + \frac{2}{3L_j^2(\Delta x)^2} + \frac{2}{3(\Delta y)^2}\right)^{-1} G^n_{i,j}, \end{aligned}\right\} \tag{9}$$

$$\left.\begin{aligned} \text{corrector:}\quad & \zeta^{n+1}_{i,j} = \zeta^n_{i,j} + \tfrac{1}{2}\Delta t(E^*_{i,j} + E^n_{i,j}), \\ & \phi^{n+1}_{i,j} = F^{n+1}_{i,j} + \tfrac{1}{2}\Delta t\left(1 + \frac{2}{3L_j^2(\Delta x)^2} + \frac{2}{3(\Delta y)^2}\right)^{-1} (G^*_{i,j} + G^n_{i,j}), \end{aligned}\right\} \tag{10}$$

where

$$\begin{aligned} E^m_{i,j} = & -\frac{1}{L_j^2(\Delta x)^2}(1+\zeta^m_{i,j})(\phi^m_{i+1,j} - 2\phi^m_{i,j} + \phi^m_{i-1,j}) - \frac{1}{4L_j^2(\Delta x)^2}(\zeta^m_{i+1,j} \\ & -\zeta^m_{i-1,j})(\phi^m_{i+1,j} - \phi^m_{i-1,j}) - \frac{1}{(\Delta y)^2}(1+\zeta^m_{i,j})(\phi^m_{i,j+1} - 2\phi^m_{i,j} + \phi^m_{i,j-1}) \\ & -\frac{1}{4(\Delta y)^2}(\zeta^m_{i,j+1} - \zeta^m_{i,j-1})(\phi^m_{i,j+1} - \phi^m_{i,j-1}) - \frac{k}{2\Delta y L_j}(1+\zeta^m_{i,j})(\phi^m_{i,j+1} - \phi^m_{i,j-1}), \end{aligned}$$

$$F_{i,j}^m = \phi_{i,j}^n + \left(1 + \frac{2}{3L_j^2(\Delta x)^2} + \frac{2}{3(\Delta y)^2}\right)^{-1} \left[\frac{1}{3L_j^2(\Delta x)^2}(\phi_{i+1,j}^m + \phi_{i-1,j}^m - \phi_{i+1,j}^n - \phi_{i-1,j}^n) + \frac{1}{3(\Delta y)^2}(\phi_{i,j+1}^m + \phi_{i,j-1}^m - \phi_{i,j+1}^n - \phi_{i,j-1}^n) + \frac{k}{6L_j\Delta y}(\phi_{i,j+1}^m - \phi_{i,j-1}^m - \phi_{i,j+1}^n + \phi_{i,j-1}^n)\right],$$

$$G_{i,j}^m = -\frac{1}{8L_j^2(\Delta x)^2}(\phi_{i+1,j}^m - \phi_{i-1,j}^m)^2 - \frac{1}{8(\Delta y)^2}(\phi_{i,j+1}^m - \phi_{i,j-1}^m)^2 - \zeta_{i,j}^m.$$

Here Δx, Δy and Δt represent spatial and temporal increments, i, j are indices denoting the spatial grid points in the x- and y-directions, respectively, and n, $*$, and $n+1$ represent different time levels of computation. The dummy variable m can be n or $*$ for E and G, and $*$ or $n+1$ for F.

We note that in (9) and (10), the values of ϕ at new time levels appear on both the left-hand side and the right-hand side of the equations. This indicates that (9) and (10) need to be solved iteratively. In our computation, at each step the values of ϕ at the previous step are used as the initial guess for the new step, and (9) and (10) are iterated until the wave field is converged, which is judged by $\max|\zeta(\text{new step}) - \zeta(\text{old step})| < \delta$ in our computations. Here δ is a small positive number that is usually chosen to be no larger than 0.1% of the $|\zeta|$ value itself. The accuracy and efficiency of the numerical scheme used in the present study will be further discussed in the next section.

4. Numerical results

Before simulating the propagation of solitary waves in curved channels, we first tested the numerical scheme on a solitary wave travelling in a straight channel of uniform depth and width. The initial condition was given by (4) with amplitude $\alpha = 0.5$. After the solitary wave had travelled for 50 non-dimensional time units or about 60 water depths, our numerical results show that the amplitude of the solitary wave increased by only 2.1%, and the changes in excess mass and mechanical energy were 0.0% and 2.1%, respectively. The error in wave speed was found to be 0.05%. These results thus validate the reasonably high accuracy of the numerical scheme.

4.1. *Solitary waves propagating through sharp-cornered 90°-bends*

In our numerical simulations, all the water channels investigated here have a single sharp-cornered 90°-bend and a total length of 200 water depths along the inner channel wall, with the upstream and downstream legs of the channel each being 100 water depths in length. The origin of the x-coordinate is set at the far upstream end of the channel. In each case, the channel width and water depth are uniform through out the channel, but the dimensionless channel width (i.e. the ratio of channel width to water depth) is varied in order to investigate the effect of channel width on transmission and reflection of solitary waves through sharp-cornered 90°-bends. For all the cases in this section, the initial position of the solitary waves is at $x_0 = 75$.

The numerical results of a solitary wave of initial amplitude $\alpha = 0.3$ propagating through a narrow channel with width $b = 1$ and with a sharp-cornered 90°-bend are shown in figure 2(*a–c*). From the results, we can see that the solitary wave is almost completely transmitted with only a small amount of reflection and scattering. It is seen that the transmitted wave is purely one-dimensional with a uniform wave crest across the channel. A detailed comparison between the transmitted and the

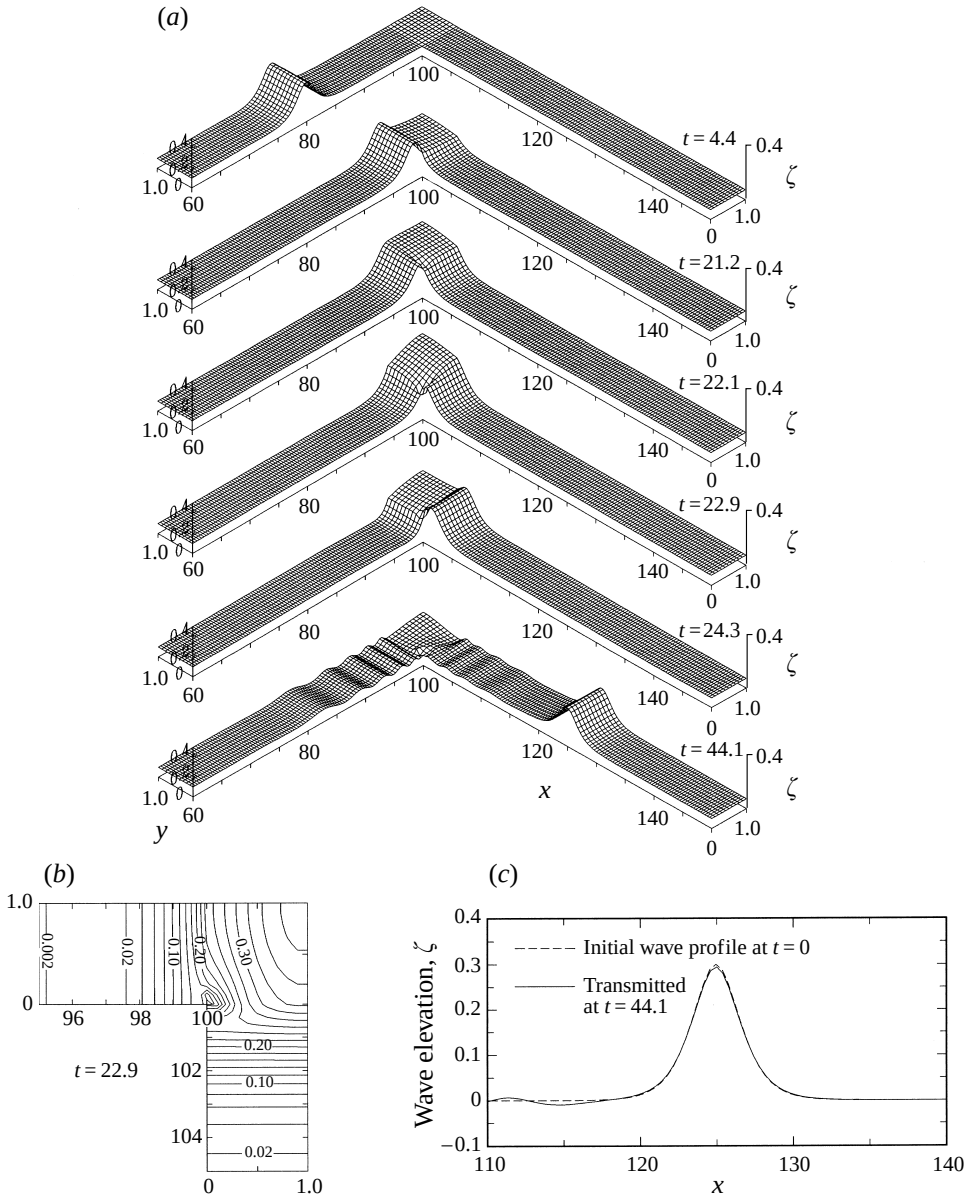

FIGURE 2. Numerical results of a solitary wave of initial amplitude $\alpha = 0.3$ and $x_0 = 75.0$ propagating through a narrow sharp-cornered 90°-bend with $b = 1$; (*a*) wave elevation at different time instants; (*b*) contour lines of the wave field at time $t = 22.9$; (*c*) comparison between the transmitted and the original wave profiles along the channel centreline.

initial wave profiles (figure 2*c*) further confirms the nearly complete transmission and preservation of the original solitary wave shape. Our numerical results show that, in this case, 99.9% of the total excess mass and 98.2% of the total energy are transmitted.

The numerical results for a solitary wave of $\alpha = 0.3$ travelling through two wider channels with $b = 5$ and 10 are shown in figures 3 and 4. We observe that the amplitude of the leading reflected wave becomes much stronger in the wider channels.

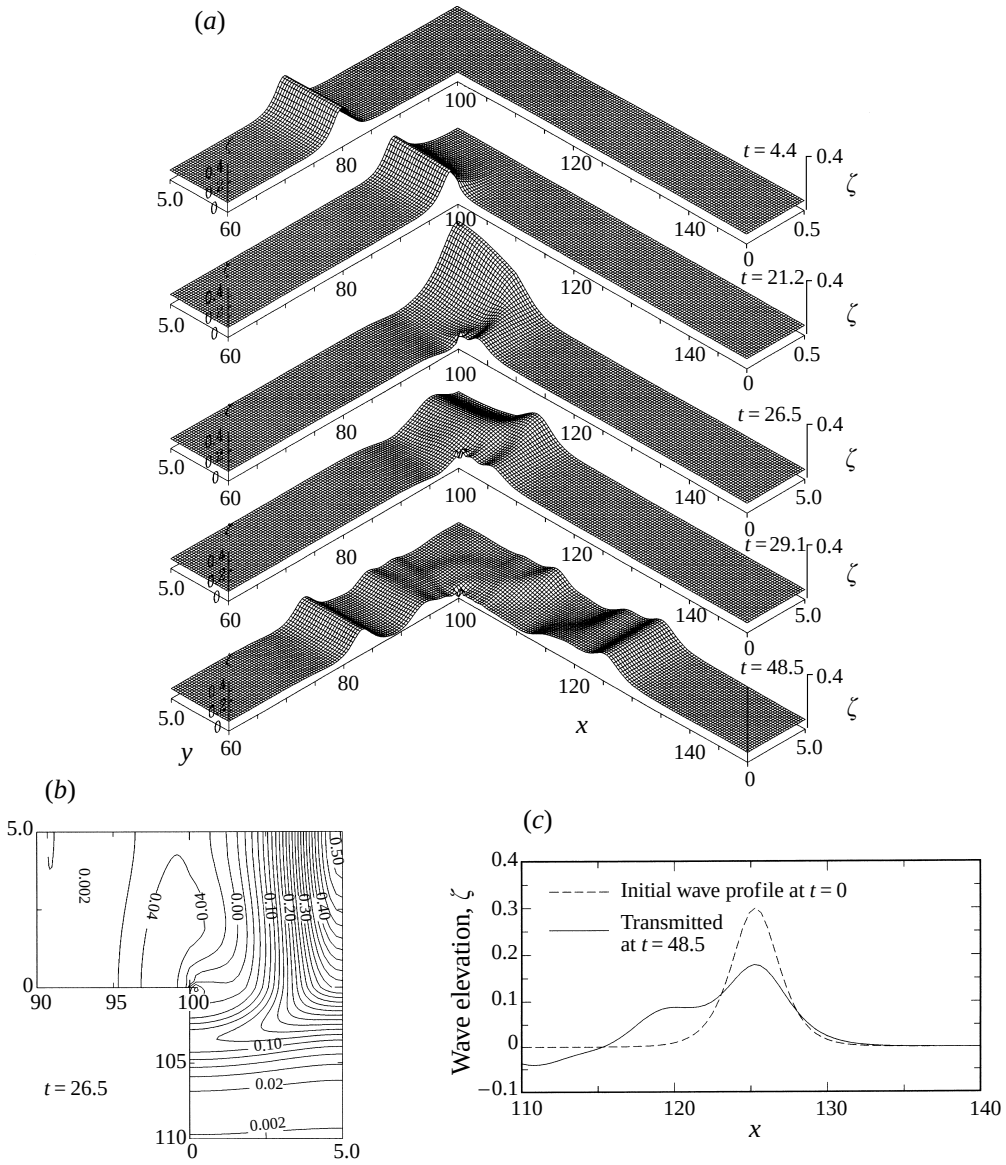

FIGURE 3. As figure 2 but with $b = 5$.

In our study, we have also simulated solitary waves of initial amplitude $\alpha = 0.3$ propagating in channels of width $b = 3$ and 7, and the detailed numerical results showing the variation of the transmitted and reflected wave amplitudes (calculated at the channel centerline) with channel width b are presented in figure 5(a, b). In this figure, the leading transmitted and reflected waves are shifted in x in order to plot all wave peaks at $x' = 0$ of the shifted x' coordinate for the convenience of comparison between waves in different channels. These results show clearly that the reflected (or transmitted) wave amplitude increases (or decreases) as channel width increases.

To further investigate the effect of channel width on wave transmission and reflection and to analyse the dominant dimensionless parameters that govern the phe-

nomenon of long waves propagating through sharp-cornered 90°-bends, we have simulated the propagation of solitary waves of different initial amplitudes $\alpha = 0.1$ and 0.5 through both narrow and wide channel bends. Our results show that the fundamental wave features with $\alpha = 0.1$ and 0.5 are very similar to those in the previous cases with $\alpha = 0.3$. Most importantly, we found that when the ratios α_T/α and α_R/α, where α_T, α_R and α represent the amplitude of the leading transmitted, reflected and the initial waves along the channel centreline, are plotted (in figure 6) against the dimensionless parameter b/λ_e, the results from all the cases with different initial wave amplitudes fall along the same curve, indicating that the ratio of channel width b to wavelength λ_e is the key similarity parameter in long-wave transmission and reflection through sharp-cornered 90°-bends.

Based on the numerical results presented in figure 6, empirical formulas for predicting the leading transmitted and reflected wave amplitudes through sharp-cornered right-angled bends with $0 < b/\lambda_e < 1$ are obtained as follows:

$$\frac{\alpha_T}{\alpha} = \begin{cases} 1, & 0 < b/\lambda_e < 0.2 \\ 0.28(b/\lambda_e)^{-0.72}, & 0.2 \leqslant b/\lambda_e < 1.0, \end{cases} \tag{11}$$

$$\frac{\alpha_R}{\alpha} = \begin{cases} 1.19(b/\lambda_e)^{0.9}, & 0 < b/\lambda_e < 0.4; \\ 0.58(b/\lambda_e)^{0.14}, & 0.4 \leqslant b/\lambda_e < 1.0, \end{cases} \tag{12}$$

where the averaged relative difference between the numerical results and the empirical approximation based on the four formulas are found to be 3%, 4%, 12% and 1%, respectively.

For solitary waves propagating through wide sharp-cornered channel bends, we also observe that the leading reflected wave appears to be very much like a solitary wave except that there is an oscillatory wave region immediately following the wave tail. Owing to the negative wave elevation which tends to cancel the excess mass possessed by the leading positive wave, the net reflected excess mass is found to be smaller than what the leading wave amplitude may suggest. For example, in the case of the solitary wave with $\alpha = 0.3$ travelling through the wide channel bend with $b = 10$, even though the reflected wave amplitude is seen to be much stronger than the transmitted wave amplitude, the transmitted excess mass M_{eT} is calculated to be 97.2% of the original total excess mass, indicating that only 2.8% of the original mass is actually being reflected. In the same case, 52.1% of the initial energy is transmitted while 47.9% is reflected. In our calculations, the reflection region is considered to include the upstream leg of the channel and the square region inside the bend, while the transmission region covers the downstream leg of the channel starting from $x = 100$. The final transmitted and reflected mass and energy are calculated at a time instant when the leading transmitted wave has travelled sufficiently far downstream of the channel bend. After that time, the transmitted and reflected mass and energy showed no significant change in time. The complex features of the reflected waves travelling in the opposite direction in comparison with the transmitted waves is the result of combined wave actions that include wave reflection due to the change in travelling direction and to the (transverse) expansion and contraction of the channel width at the bend, and due to wave diffraction around the sharp corner. Since oscillatory wave trains can have large energy but possess little net excess mass, wave energy seems to be a better measure of the intensity of the reflected waves in this case. Figure 7(a, b) shows the detailed numerical results of the ratio of transmitted and reflected excess mass M_{eT}, M_{eR} and energy E_T, E_R to the original excess mass M_e and energy E, respectively, of all the cases studied here. Again, we find that the

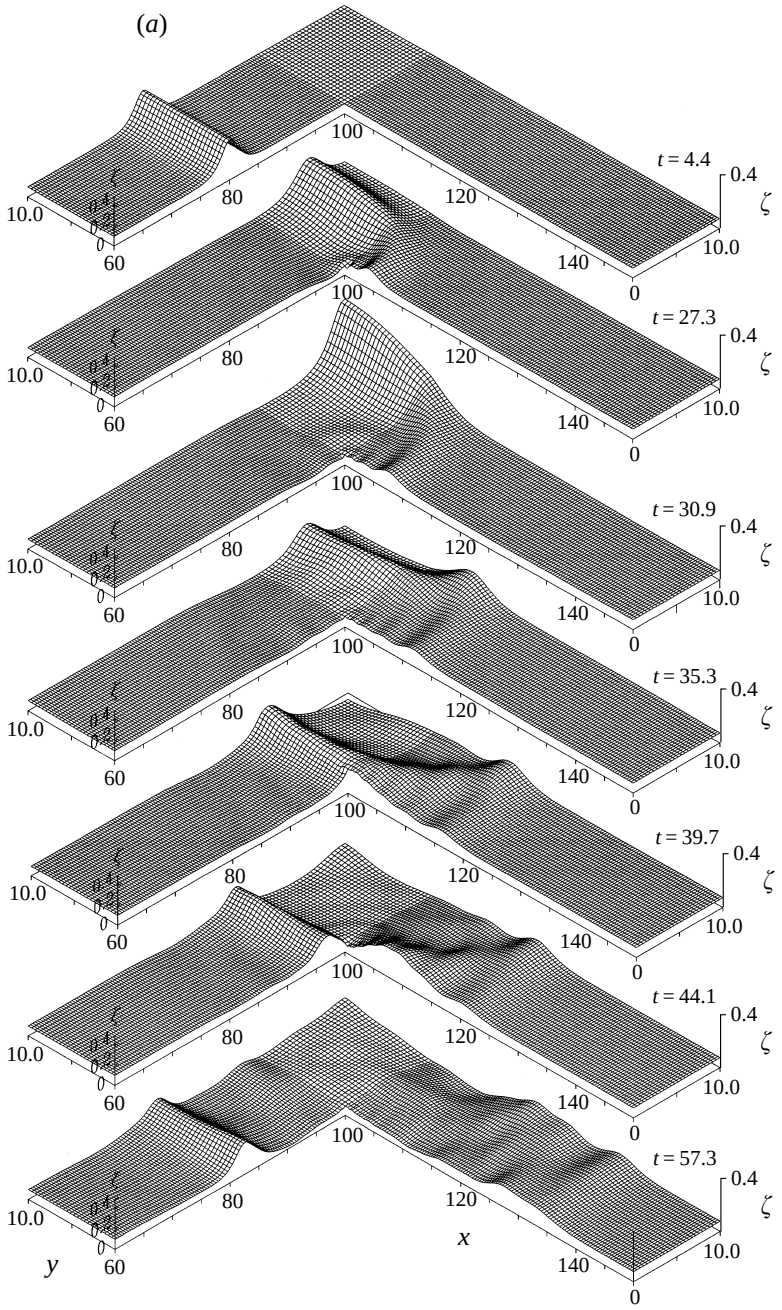

FIGURE 4(*a*). For caption see facing page.

relative transmitted and reflected mass and energy for all amplitudes depend on one dimensionless parameter, namely the ratio of channel width b to wavelength λ_e.

4.2. *Solitary waves propagating through smoothly curved 90°-bends*

For solitary waves travelling through smoothly curved channels, the first case we investigated is a solitary wave of initial amplitude $\alpha = 0.3$ at position $x_0 = 85$

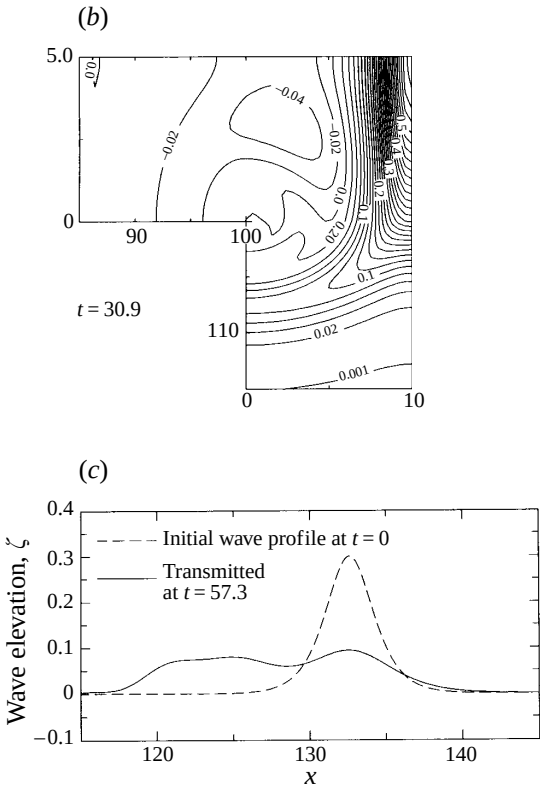

FIGURE 4. As figure 2 but with $b = 10$.

propagating through a smoothly curved narrow ($b = 1$) 90°-bend with constant radius $R = 10$ and bending sharpness $a = 1.1$. The numerical results for this case are presented in figure 8(*a–c*) showing the evolution of the solitary wave at different time instants through the 90°-bend. These results show that during its passage through a smooth bending narrow channel, a solitary wave exhibits the conspicuous features that its crest turns radially straight and tilts higher outward against the outer wall in keeping balance with the centrifugal force. After exiting from the channel bend, the solitary wave quickly regains its original shape and speed, leaving no trace of reflected waves behind.

The results for solitary waves of initial amplitude $\alpha = 0.3$ and position $x_0 = 85$ propagating through wider smooth channel bends with $b = 5$, $R = 10$, $a = 1.5$ and $b = 10$, $R = 10$, $a = 2$ are shown in figures 9 and 10. These results show that the crest of the solitary wave in a wide channel bend is no longer radially straight, and the transmitted wave no longer preserves the original shape of a solitary wave. Instead, the transmitted wave is seen to have disintegrated into several smaller waves whose elevation varies across the channel. However, even though the transmitted wave no longer preserves its original shape, it is interesting to note that, in all cases with smooth channel bends studied here, the waves are transmitted almost completely, with no significant wave reflection detected. This feature is different from that for waves propagating through sharp-cornered wide channel bends.

To examine the flow variations in the transverse direction, plots of wave elevation ζ and longitudinal fluid velocity u across the channel inside the channel bends for

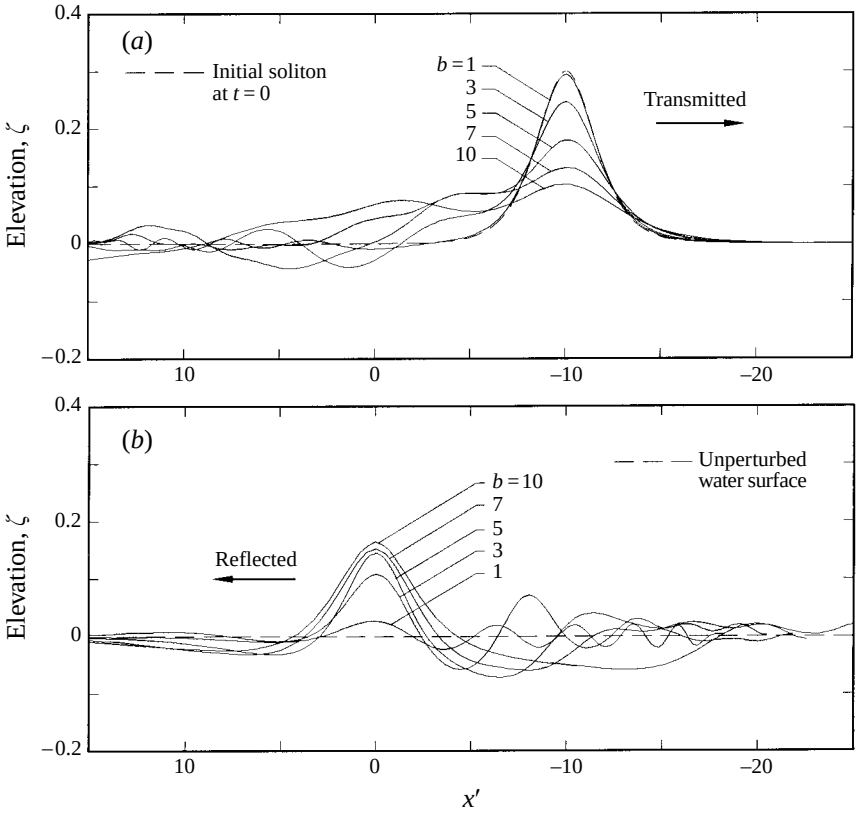

FIGURE 5. Numerical results of transmitted and reflected wave amplitudes with channel width b for a solitary wave of initial amplitude $\alpha = 0.3$ travelling through sharp-cornered 90°-bends: (*a*) transmitted waves; (*b*) reflected waves.

all three cases discussed above and an additional case with $\alpha = 0.3$, $b = 1$ and $R = 2$ (which gives $a = 1.5$) are shown in figure 11(a, b). The wave elevation ζ and velocity u shown here are taken around midway inside the channel bends where the flow variations in the transverse direction appear to be the most significant. For a solitary wave travelling through the two smooth narrow bends with $b = 1$, the wave-induced fluid velocity u is found to decrease inversely with the local radius $r = R + y$, the same as the velocity distribution of an inviscid vortex confined between two concentric cylindrical walls. This result is consistent with the result reported by Rostafinski (1972) for long acoustic waves propagating in smoothly curved narrow ducts. In contrast, for waves travelling through wide channel bends with $b = 5$ and 10, we found that the tangential fluid velocity is no longer proportional to the inverse of the local radius; instead, it increases from the inner wall to the outer wall, showing a trend similar to the typical velocity distribution in a wide river bend.

Another issue of interest is the effect of channel bends on wave speed. To calculate the averaged wave speed throughout the passage of a solitary wave in a curved channel, we define the averaged wave speed as the total longitudinal distance travelled along the channel centreline divided by the corresponding travel time. For all cases presented in §4.1 and §4.2, we calculated the average wave speed from the initial wave position, which is about one wavelength upstream of the channel bend, to where the tail of the leading transmitted wave has travelled out of the bend. To examine

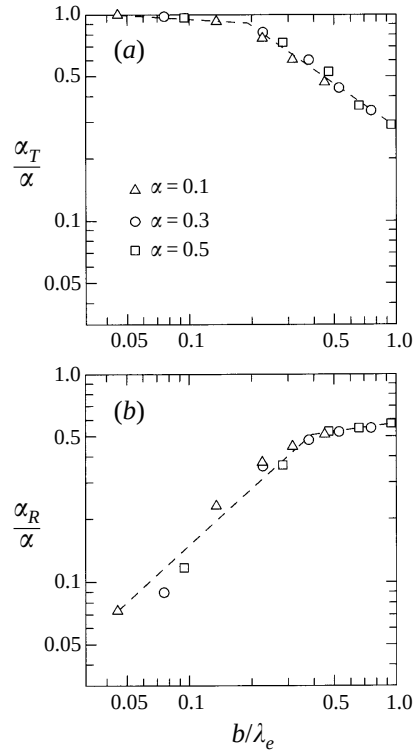

FIGURE 6. Plot of the ratio of (*a*) transmitted and (*b*) reflected wave amplitude α_T and α_R to the initial amplitude α vs. the ratio of channel width b to wavelength λ_e with logarithmic axes.

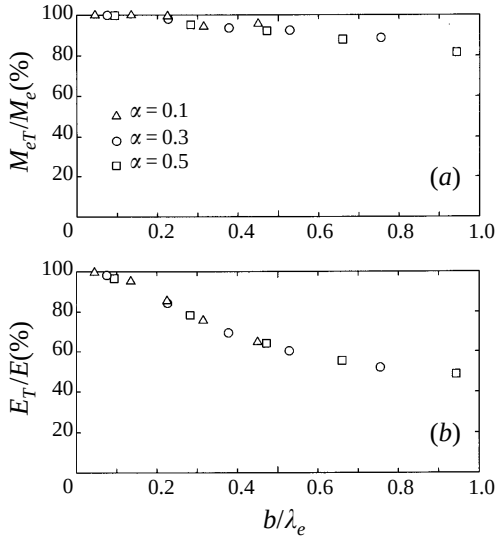

FIGURE 7. Numerical results of transmitted (*a*) excess mass M_{eT} and (*b*) mechanical energy E_T for a solitary wave of initial amplitude α travelling through sharp-cornered 90°-bends, where M_e and E are initial excess mass and mechanical energy, and b and λ_e are channel width and effective wavelength, respectively.

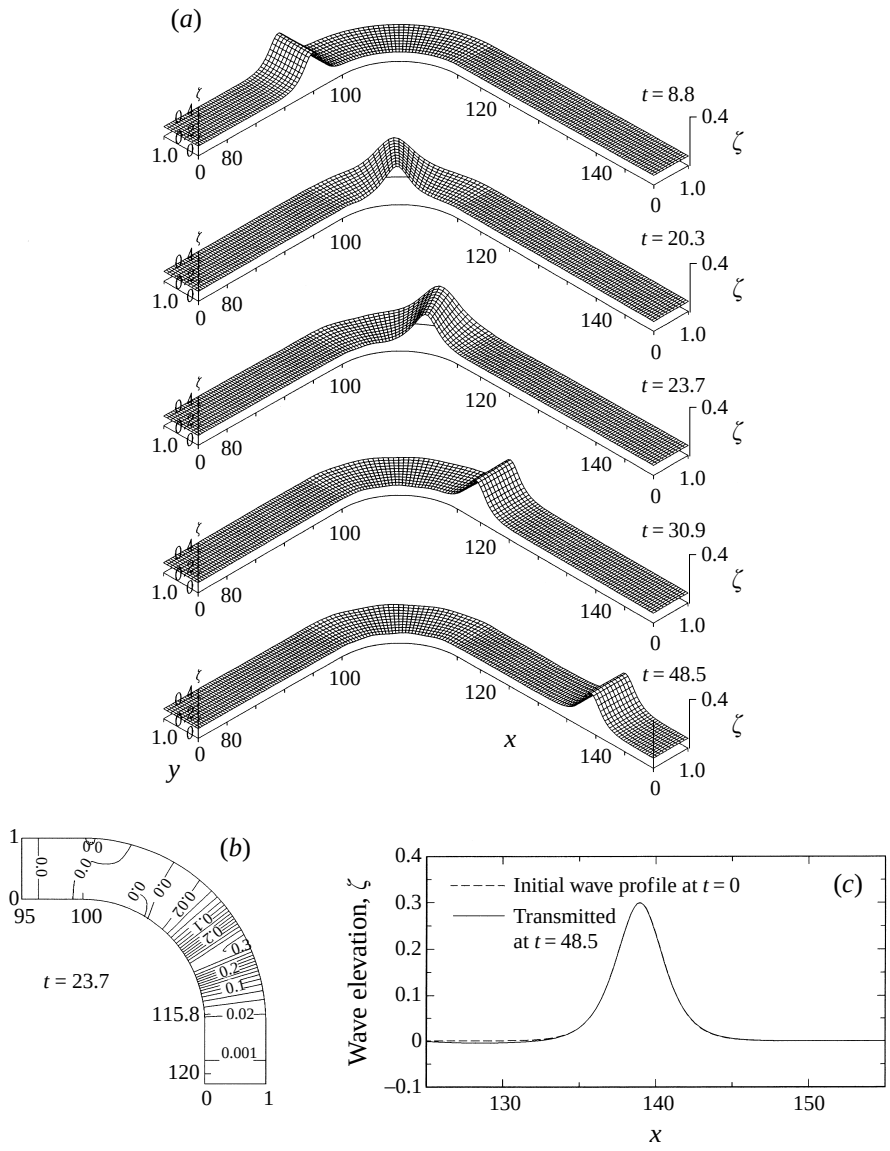

FIGURE 8. Numerical results of a solitary wave with initial amplitude $\alpha = 0.3$ and $x_0 = 85.0$ travelling through a narrow smoothly curved 90°-bend with $b = 1$, $R = 10$, and $a = 1.1$: (*a*) wave elevation at different time instants; (*b*) contour lines of the wave field at time $t = 23.7$; (*c*) comparison between the transmitted and the original wave profiles along the channel centreline.

the effect of channel bend on wave speed, the numerical results for wave speed in curved channels are compared with the speed calculated by using (5) for waves travelling in a straight channel, with α in (5) taken as the average of the initial wave amplitude and the amplitude of the leading transmitted wave. Detailed results for wave speed in both the smoothly curved channels and channels with sharp-cornered bends are presented in tables 1 and 2. In these tables, x_0, α, x, α_T, $\bar{\alpha}$, $c_{(5)}$, c, and diff.% represent, respectively, the initial wave position, the initial wave amplitude, the final wave position, the amplitude of the leading transmitted wave, the averaged amplitude

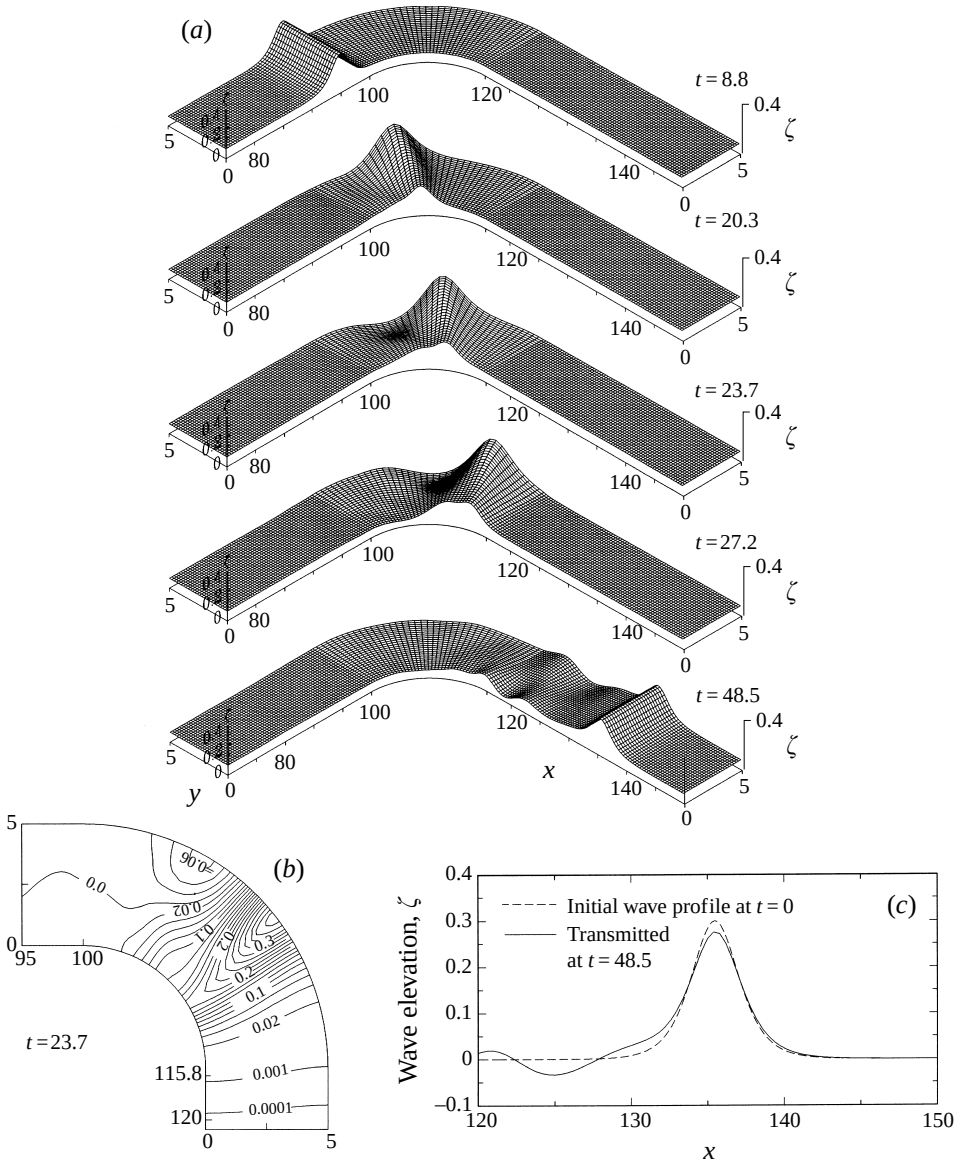

FIGURE 9. As figure 8 but with $b = 5$, and $a = 1.5$.

0.5 $(\alpha + \alpha_T)$, the wave speed in straight channels based on $\bar{\alpha}$ calculated from (5), the actual wave speed in curved channels, and the relative difference between $c_{(5)}$ and c.

Our results show that the averaged wave speed for a solitary wave travelling through a smoothly curved channel of constant depth is almost the same as that in a straight channel given by (5). Comparing the cases with narrow and wide channel bends with sharpness a ranging from 1.1 to 2, we find that the bend sharpness a has little effect on the averaged wave speed in smoothly curved channels. For solitary waves travelling through sharp-cornered 90°-bends, the wave speed is seen to be slightly faster than that in a straight channel based on the same wave amplitude and same travel length. The difference is quite small, except in the case of the wide

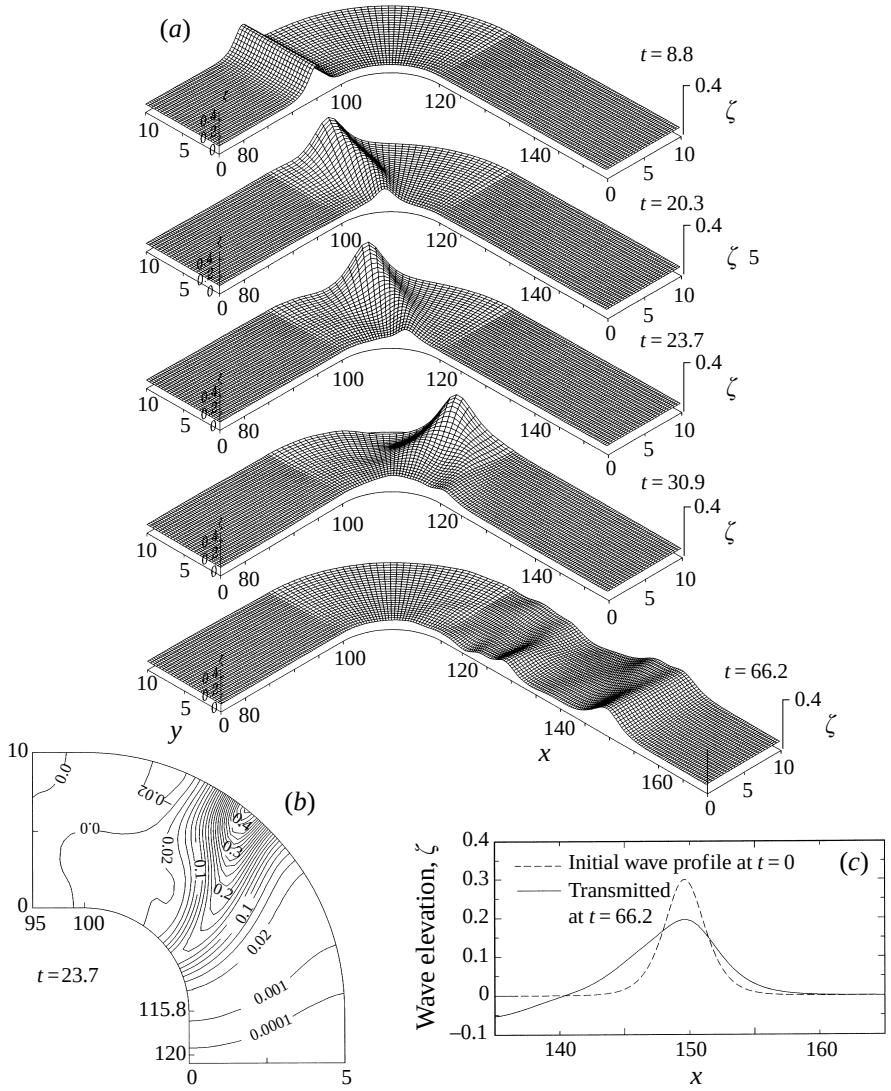

FIGURE 10. As figure 8 but with $b = 10$, and $a = 2.0$.

channel with $b = 10$. However, in this case, the amplitude of the transmitted wave has decreased so much compared with the initial wave amplitude that it may not be meaningful to compare the wave speed with the one calculated by using (5) based on the averaged wave amplitude.

In our computations, the typical values we used for Δx, Δy and Δt are 0.1, 0.1 and 0.05, respectively, and the convergence criterion δ is set to $\delta = 0.001|\zeta|$. We have also tested the conditionally stable scheme by using $\Delta x = \Delta y = 0.2$, $\Delta t = 0.05$ and $\Delta x = \Delta y = 0.05$, $\Delta t = 0.05$ and obtained the same results. (The minimum iteration number is different for different Δx, Δy and Δt.) The conservation of excess mass and mechanical energy was monitored in all our computations, and the maximum errors in mass and energy conservation in all our simulations of waves propagating through

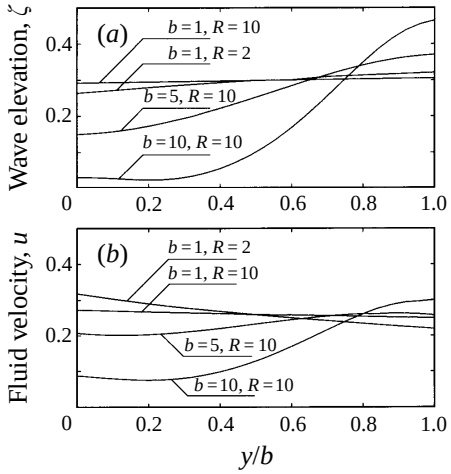

FIGURE 11. Numerical results showing the variations of (*a*) wave elevation ζ and (*b*) longitudinal fluid velocity u across the channel width inside the smoothly curved 90°-bends about halfway around the bend. The amplitude of the initial solitary wave is $\alpha = 0.3$.

Width b	Sharpness a	x_0	α	x	α_T	$\bar{\alpha}$	$c_{(5)}$	c	Diff.%
1	1.1	85	0.3	139	0.299	0.3	1.134	1.133	0.1
1	1.5	85	0.3	139	0.299	0.3	1.134	1.131	0.3
5	1.5	85	0.3	136	0.276	0.288	1.129	1.122	0.6
10	2.0	85	0.3	149	0.196	0.248	1.113	1.093	1.8

TABLE 1. Wave speed c in smoothly curved channels

Width b	x_0	α	x	α_T	$\bar{\alpha}$	$c_{(5)}$	c	Diff.%
1	75	0.3	125	0.294	0.297	1.133	1.154	1.9
5	75	0.3	125	0.181	0.240	1.109	1.142	3.0
10	75	0.3	133	0.102	0.201	1.093	1.183	8.2

TABLE 2. Wave speed c in channels with sharp-cornered 90°-bends

both smooth and sharp-cornered bends were 1.2% for M_e and 4.1% for E. A typical case in our numerical simulation uses about 46 minutes of CPU time on a Cray c90.

5. Discussion

Our present numerical results revealed very similar behaviours of solitary waves travelling through narrow curved channels and long acoustic waves in narrow bending ducts studied by Rostafinski (1972). The similarity lies in that a long wave is transmitted almost completely in a narrow curved channel with little backward reflection, and the tangential fluid velocity inside a smooth circular-arc bend is proportional to the inverse of the local radius in the transverse direction, same as the velocity distribution of a potential vortex. Rostafinski's (1972) analytical solution based on the linear wave equations predicted that wave speed would increase as bending sharpness increases. Even though this effect is not apparent in our present results for solitary waves in smoothly curved channels, our results indicated that the wave speed is slightly

faster through a sharp-cornered 90°-bend than that in a straight channel. The consistency between our numerical results for long water waves in narrow curved channels and Rostafinski's analytical solution for long acoustic waves in narrow curved ducts further validates the correctness of the numerical scheme and our simulation results.

In the present study, new results are obtained for solitary waves travelling in wide channels. As we noted, the wave behaviour through narrow smoothly curved and sharp-cornered channel bends is very similar: in other words, for narrow curved channels, the bending sharpness is not an important parameter. However, the transmission and reflection of solitary waves through wide smoothly curved and sharp-cornered bends are seen to be very different. We observe that when travelling through wide sharp-cornered 90°-bends, wave reflection is very significant, whereas through a wide smoothly curved channel bend, the initial wave is fully transmitted with no backward reflection. This result can be useful in predicting and controlling wave transmission and reflection in hydraulic engineering applications.

The maximum channel width we examined in the present study is ten times the water depth. Waves in much wider channels are not simulated because the gB model is a depth-averaged shallow water model and may not be applicable to modelling waves in extremely wide channel bends where secondary flow may occur.

Although there is no backward reflection of a solitary wave travelling through a wide smooth channel bend, there seems to be a noticeable lateral reflection from the outer channel wall inside the bend which causes the initial wave to disintegrate into several smaller waves whose elevation varies across the channel. This reflection from the outer wall in wide channels is qualitatively consistent with the effect of channel walls on short waves as reported by Kirby *et al.* (1994). However, since long and short waves have different characteristics, their behaviour in curved channel bends may not be compared quantitatively.

It will be interesting and valuable to conduct laboratory experiments to further investigate the phenomenon of solitary waves propagating through curved and branching channels. A sharp-cornered right-angled channel is currently being set up in the hydraulics lab at the University of Hawaii. Quantitative measurements of wave transmission and reflection are being planned. We are particularly interested in examining the similarity relationships (11), (12) between the relative transmitted or reflected wave amplitude and the ratio of channel width to wavelength, which are revealed by our present numerical results.

Another problem of interest is the propagation of solitary waves in branching channels. In Shi & Teng (1996), solitary waves travelling through a T-shaped narrow branching channel were studied. Extending the study to include wide branching channels with general branching angles is currently being pursued.

6. Conclusion

The generalized nonlinear and dispersive Boussinesq model (Wu 1981) was computed numerically to simulate the propagation of solitary waves in channels with smoothly curved and sharp-cornered 90°-bends. Our numerical results show that when travelling through narrow channel bends, including both smoothly curved and sharp-cornered bends, a solitary wave is transmitted almost completely with little reflection and scattering. The longitudinal fluid velocity inside a smoothly curved circular-arc narrow bend is found to vary inversely with the local radius across the channel, the same as the velocity distribution of a potential vortex and also consistent

with the results for long acoustic waves in smoothly curved narrow ducts (Rostafinski 1972).

For solitary waves travelling through wide smoothly curved channels, our results show that the initial wave is fully transmitted without backward reflection. However, in this case, the transmitted wave no longer preserves the shape of the original solitary wave but disintegrates into several smaller waves due to lateral reflection from the outer channel wall. In addition, the longitudinal fluid velocity inside a wide smooth bend is no longer proportional to the inverse of the local radius; instead, it increases from the inner wall to the outer wall. We also found that, the speed of solitary waves propagating through smoothly curved channels is the same as that in a straight channel.

For a solitary wave travelling through a wide channel with a sharp-cornered 90°-bend, the backward reflection is seen to be very significant, and the wider the channel bend, the stronger the reflected wave amplitude. A similarity relationship is revealed by our numerical results: the relative transmitted and reflected wave amplitude, excess mass and energy, scaled by the original amplitude, mass and energy, all depend on one single dimensionless parameter, namely the ratio of the channel width b to the effective wavelength λ_e. This result not only helped to reveal the key similarity parameter (i.e. b/λ_e) that governs the transmission and reflection of solitary waves through sharp-cornered bends, but also helped us to obtain simple power laws for predicting the transmitted and reflected wave amplitudes based on b/λ_e. Regarding the wave speed, solitary waves are observed to travel slightly faster in a channel with a sharp-cornered bend than in a straight channel.

The authors wish to thank Professor Allen Chwang at the Hong Kong University, Professor Philip Liu at Cornell University and Professor Harry Yeh at the University of Washington for providing us with their valuable comments. The authors appreciate greatly the helpful discussions with Professors C. C. Mei, R. Grimshaw, C.-S. Yih, S. J. Lee, and S. H. Kwon at the 2nd International Conference on Hydrodynamics in Hong Kong. We are also grateful to the reviewers for their helpful comments, especially for those on the effect of wavelength and on the important results by Rostafinski (1972, 1976) and by Kirby *et al.* (1994). Computations in the present study were performed on Cray c90 at the San Diego Supercomputer Center (SDSC) which is supported by the US National Science Foundation.

REFERENCES

Benjamin, T. B. 1972 The stability of solitary waves. *Proc. R. Soc. Lond.* A **328**, 153–183.

Chang, P., Melville, W. K. & Miles, J. W. 1979 On the evolution of a solitary wave in a gradually varying channel. *J. Fluid Mech.* **95**, 401–414.

Goring, D. G. 1978 Tsunamis – The propagation of long waves onto a shelf. *Rep.* KH-R-38. Keck Laboratory, California Institute of Technology, Pasadena, California.

Johnson, R. S. 1973 On the development of a solitary wave moving over an uneven bottom. *Proc. Camb. Phil. Soc.* **73**, 183–203.

Katopodes, N. D. & Wu, C.-T. 1987 Computation of finite-amplitude dispersive waves. *ASCE J. Waterway, Port, Coastal & Ocean Engng* **113**, 327–346.

Kirby, J. T., Dalrymple, R. A. & Kaku, H. 1994 Parabolic approximations for water waves in conformal coordinate systems. *Coastal Engng* **23**, 185–213.

Kirby, J. T. & Vengayil, P. 1988 Nonresonant and resonant reflection of long waves in varying channels. *J. Geophys. Res.* **39**, 10782–10796.

Madsen, O. S. & Mei, C. C. 1969 The transformation of a solitary wave over an uneven bottom. *J. Fluid Mech.* **39**, 781–791.

Miles, J. W. 1979 On the Korteweg-de Vries equation for a gradually varying channel. *J. Fluid Mech.* **91**, 181–190.

Peregrine, D. H. 1967 Long waves on a beach. *J. Fluid Mech.* **27**, 815–827.

Rostafinski, W. 1972 On propagation of long waves in curved ducts. *J. Acoust. Soc. Am.* **52**, 1411–1420.

Rostafinski, W. 1976 Acoustic systems containing curved duct sections. *J. Acoust. Soc. Am.* **60**, 23–28.

Schember, H. R. 1982 A new model for three-dimensional nonlinear dispersive long waves. PhD thesis, California Institute of Technology, Pasadena, California.

Shi, A. & Teng, M. H. 1996 Propagation of solitary wave in channels of complex configurations. In *Proc. 2nd Intl Conf. on Hydrodynamics.* (ed. A. T. Chwang, J. H. Lee & D. Y. Leung), pp. 349–354. Balkema, Rotterdam.

Shuto, N. 1974 Nonlinear long waves in a channel of variable section. *Coastal Engng Japan* **17**, 1–12.

Teng, M. H. 1990 Forced emissions of nonlinear water waves in channels of arbitrary shape. PhD thesis, California Institute of Technology, Pasadena, California.

Teng, M. H. 1997 Solitary wave solution to Boussinesq equations. Technical Note, *ASCE J. Waterway, Port, Coastal Ocean Engng* **123**, 138–141.

Teng, M. H. & Wu, T. Y. 1992 Nonlinear water waves in channels of arbitrary shape. *J. Fluid Mech.* **242**, 211–233.

Teng, M. H. & Wu, T. Y. 1994 Evolution of long water waves in variable channels. *J. Fluid Mech.* **266**, 303–317.

Wang, K. H., Wu, T. Y. & Yates, G. T. 1988 Scattering and diffraction of solitary waves by a vertical cylinder. In *Proc. 17th Symp. on Naval Hydrodynamics*, pp. 37–46. The Hague, The Netherlands.

Wang, K. H., Wu, T. Y. & Yates, G. T. 1992 Three-dimensional scattering of solitary waves by vertical cylinder. *ASCE J. Waterway, Port, Coastal and Ocean Engng* **118**, 551–566.

Webb, A. J. & Pond, S. 1986 The Propagation of a Kelvin wave around a bend in a channel. *J. Fluid Mech.* **169**, 257–274.

Wu, T. Y. 1981 Long waves in ocean and coastal waters. *ASCE J. Engng. Mech.* **107**, 501–522.

Yates, G. T. 1995 Various Boussinesq solitary wave solutions. In *Proc. 5th Intl Offshore and Polar Engng. Conf.*, pp. 70–76. The Intl Soc. Offshore and Polar Engineers.

Zabusky, N. J. & Kruskal, M. D. 1965 Interaction of solitons in a collisionless plasma and the recurrence of initial states. *Phys. Rev. Lett.* **15**, 240–243.